

Analysis of B–SiO₂ films by highly charged ion based time-of-flight secondary ion mass spectrometry, standard secondary ion mass spectrometry and elastic recoil detection

T. Schenkel,^{a)} A. V. Hamza, A. V. Barnes, and D. H. Schneider
Lawrence Livermore National Laboratory, Livermore, California 94550

D. S. Walsh and B. L. Doyle
Physics Department, Sandia National Laboratory, S. E., Albuquerque, New Mexico 87185-1056

(Received 14 October 1997; accepted 9 February 1998)

B–SiO₂ films formed by chemical vapor deposition on silicon substrates were analyzed by time-of-flight secondary ion mass spectrometry using slow Xe⁴⁴⁺ and Th⁷⁰⁺ as primary ions. Boron concentrations of $2 \times 10^{21} \text{ cm}^{-3}$ determined directly from positive secondary ion spectra agree with results from elastic recoil detection measurements, indicating strong decoupling of positive secondary ion production probabilities from elemental ionization potentials in the intense electronic sputtering induced by highly charged ions. Results demonstrate advantages of highly charged ions for quantitative analysis of surface near layers of materials. © 1998 American Vacuum Society. [S0734-2101(98)04703-4]

I. INTRODUCTION

Quantitative analysis of surfaces and thin films is a crucial problem in materials research. Quantitative accuracy, sensitivity, and depth resolution of secondary ion mass spectrometry (SIMS) have been optimized continuously over the last decades. In dynamic SIMS, limits in quantitative accuracy due to changing secondary ion production probabilities as a function of chemical environment (“matrix effects”) have been addressed by preparation of constant ionization environments, e.g., through use of oxygen ion beams and flooding of samples with oxygen during depth profiling.^{1,2} It has been shown that monitoring of MCs⁺ molecular ions during Cs⁺ bombardment is largely unaffected by changing matrices.³ Use of lasers for resonant⁴ or non-resonant⁵ positionization of secondary neutrals marks another route to quantitative compositional analysis. Useful yields, i.e., the number of secondary ions detected per sputtered target atom, are typically in the order of 10^{-2} (Refs. 4, 6, and 7) and can be as low as 10^{-6} . Accurate quantification often has to rely on the use of calibration standards or make use of cross calibration with independent analytical techniques.⁸

Recently, strong electronic sputtering effects were reported for impact of slow ($\sim 1 \text{ keV/u}$) highly charged ions, like Xe⁴⁴⁺ and Au⁶⁹⁺, on thin insulating films and semi-metallic foils.^{9,10} Atomic and molecular secondary ion yields were found to be increased by over two orders of magnitude for highly charged as compared to singly charged ions at the same kinetic energy.⁹ In the case of Au⁶⁹⁺ on B–SiO₂ (50 nm on Si), at average more than three secondary ions were detected per incident highly charged ion. In this article we report on the first application of highly charged ion induced electronic sputtering for quantitative materials analysis.

II. EXPERIMENT

Highly charged ions were extracted from the LLNL Electron Beam Ion Trap (EBIT).¹¹ The setup for highly charged

ion based time-of-flight secondary ion mass spectrometry (TOF-SIMS) has previously been described in detail.⁹ In short, secondary electrons or protons, emitted at impact of individual ions, are used to start time-of-flight cycles. Start efficiencies were 100% for electron starts and typically $>50\%$ for proton starts. Negative or positive secondary ions are detected in a micro-channel-plate detector and are accepted as stops in a multistop time analyzer [ORTEC 9308]. Secondary ions are accelerated by a target bias of $\pm 3 \text{ kV}$. The flight path has a length of only 10 cm. The resulting mass resolution was limited to $m/\Delta m = 100$. Targets consisted of 50 nm thick B–SiO₂ films deposited on silicon substrates by standard plasma enhanced chemical vapor deposition (PE-CVD). The intensity of achievable highly charged ion beams from EBIT is currently limited to $\leq 10^6$ ions/s on a spot of $\sim 1 \text{ mm}^2$. For depth profiling, targets were thus eroded by conventional low energy ion sputtering (3 keV Ar^{1+} , at normal impact, rastered over 1 cm^2) and highly charged ions were used to analyze targets after subsequent sputtering cycles. Sputter depths were calculated from the Ar-sputter ion dose using literature values for sputter yields.¹² Resulting depth scales were consistent with determinations of the point of interface crossing to the Si substrate by monitoring of characteristic molecular ions, like SiO₃[−]. Re-absorption from the residual gas provided sufficient hydrogen for efficient generation of start signals in TOF-SIMS of positive secondary ions. Additionally, hydrogen could be bled onto the target if needed. Accumulation times for TOF-SIMS spectra were typically $\sim 10 \text{ min}$. At the highly charged ion beam intensities of 10^3 – 10^4 ions per second which were used for TOF-SIMS, this corresponds to static conditions where only insignificant amounts of target material are removed. The dynamic range currently achievable with the single detector TOF-setup spanned only ~ 3 orders of magnitude. The dominant background source were

^{a)}Electronic mail: SCHENKEL2@LLNL.GOV

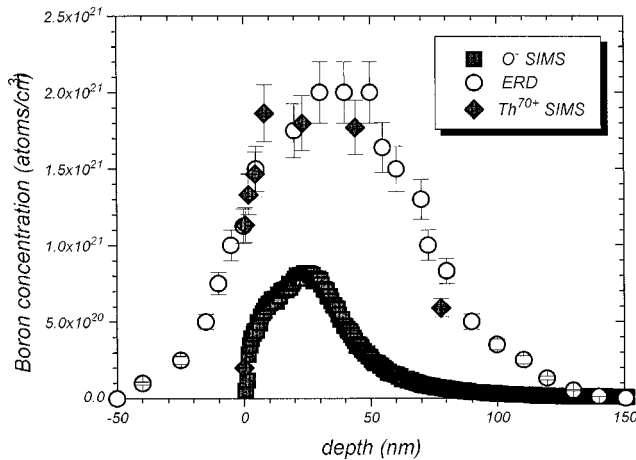


FIG. 1. Boron concentration in the B-SiO₂/Si films as determined by highly charged ion based TOF-SIMS (◆), elastic recoil detection (○), and standard SIMS (■).

uncorrelated coincidences between starts and signals from subsequent primary ions striking the target before the end of a time-of-flight cycle.

B-SiO₂ targets were analyzed by elastic recoil detection (ERD)¹³ at Sandia National Laboratory using a beam of 24 MeV Si⁵⁺ in order to independently determine the absolute boron concentrations. A CAMECA 4*f* magnetic sector instrument was used for standard SIMS measurements. Primary ions were O⁻ at an effective kinetic energy of 17 keV. The angle of incidence was ~25°. The beam spot diameter was ~20 μm, rastered over an area of ~100 μm×100 μm.

III. RESULTS AND DISCUSSION

Figure 1 shows resulting boron depth profiles from highly charged ion based TOF-SIMS, ERD, and standard SIMS. The peak concentration of boron in the films as determined by ERD was 2×10^{21} atoms/cm³. Probe beams for highly charged ion based TOF-SIMS were Xe⁴⁴⁺ (first two data points) and Th⁷⁰⁺ at kinetic energies of 1.3 and 1.2 keV/u, respectively, and at normal incidence. The probe beam was switched in order to take advantage of increased secondary ion yields as a function of primary ion charge.⁹ For determination of boron concentrations from positive secondary ion spectra, the number of counts in the ¹¹B⁺ and ¹⁰B⁺ peak areas was divided by the integrated positive secondary ion counts from the matrix after background subtraction. The average fractional boron content in the broad maximum of the distribution was 2.8 at. %. At a given atomic density of the SiO₂ matrix of $\sim 6.6 \times 10^{22}$ atoms/cm³ we find that results from ERD (fractional boron content: 3 at. %) and TOF-SIMS (boron concentration: 1.8×10^{21} atoms/cm³) agree within the uncertainty of the measurements of $\pm 10\%$. In standard SIMS, ¹¹B⁺ and ³⁰Si⁺ ions were recorded as a function of sputtering time. Boron concentrations were calculated directly from measured ¹¹B⁺ to ³⁰Si⁺ count ratios without correction for different ionization probabilities of boron and silicon and assuming an atomic density of the SiO₂ matrix of 6.6×10^{22} atoms/cm³. The value of the boron peak concen-

tration was thus determined to be only 0.8×10^{21} atoms/cm³. Standard SIMS underestimates the true concentration by over a factor of ~ 2.5 . Quantitatively accurate concentrations can be derived from standard SIMS data using calibrated standards or cross calibration with independent analytical techniques.⁸

Depth resolution in standard and highly charged ion based SIMS is determined by low energy ion sputtering parameters. Optimization of depth resolution was not pursued in this study. Separating mass removal from probing in highly charged ion based SIMS, however, allows for optimization of depth profiling conditions independent of concerns of efficient secondary ion formation.¹⁴

Slow, highly charged ions impose conditions of extreme target ionization upon impact on a nanometer sized surface area. Over one hundred electrons are emitted from thin SiO₂ films at impact of individual Th⁷⁰⁺.⁹ The target lattice reacts to the intense Coulomb stress by emission of high amounts of charged⁹ and neutral¹⁵ secondary particles. Positive secondary ion spectra are dominated by singly positively charged atomic ions.⁹ We interpret the good agreement of boron concentration measurements by ERD and highly charged ion based TOF-SIMS as resulting from strong decoupling of positive secondary ion production probabilities from elemental ionization potentials under conditions of electronic sputtering induced by highly charged ions.¹⁶ In standard SIMS, production of atomic secondary ions is dominated by elemental ionization potentials, p^+ , and the chemical environment of the matrix. Ionization probabilities have been quantified in studies of relative sensitivity factors (RSF).¹⁷ Ionization potentials of Si (8.15 eV) and B (8.23 eV) are very similar and the RSF for boron in a silicon or SiO₂ matrix under oxygen bombardment has been found to be 6.5×10^{22} (cm⁻³), indicating that detection of positive secondary ions allows for accurate determination of actual concentrations of boron in these matrices. RSF factors are determined by use of implantation standards with impurity concentrations typically much lower than the atomic percent range present in the samples used in this study. Our results show that RSF factors in standard SIMS are affected by very high impurity concentrations, where the influence of the impurity on the chemical structure of the matrix is not negligible as it is for fractional impurity concentrations $< 0.1\%$. From our measurements the RSF for the detection of boron in SiO₂ at concentrations in the atomic percent range follows to be 1.6×10^{23} (cm⁻³) for SIMS using O⁻ primary ions. For highly charged ion based SIMS the RSF is 6.6×10^{22} (cm⁻³).

Accurate quantitative analysis of near surface dopant concentrations in the atomic percent range is of significant technological relevance as these distributions are present in the low energy (< 5 keV) implants used for ultrashallow junction formation.

The matrix stoichiometry of the B-SiO₂ films was confirmed to be 2:1 by Rutherford backscattering. This ratio was not reproduced in the ratio of oxygen to silicon positive secondary ion yields in highly charged ion based SIMS, which

was found to be only $0.8 (\pm 0.05)$. We note that the comparably large difference in ionization potentials between oxygen (13.6 eV) and silicon results in secondary ion yield variations by several orders of magnitude under standard SIMS conditions.¹⁷ The deviation in oxygen and silicon ion yields from the true stoichiometry can be attributed in part to secondary ion formation at the fringe of the highly charged ion impact area, where the ionization density is gradually decreasing and the influence of ionization potentials begins to dominate ionization probabilities. In an ongoing study, decoupling of secondary ion production probabilities from ionization potentials was also observed for submonolayer iron ($p^+_{\text{Fe}}=7.9$ eV) coverages on graphite samples ($p^+_C=11.26$ eV). Here fractional concentrations of (7.7 ± 0.5) at. % were found using Xe^{44+} , while analysis using the Sandia heavy ion backscattering system¹⁸ showed a fractional concentration of (6.8 ± 0.7) at. %.

Complementary to atomic, positive secondary ions, spectra of molecular secondary ions in highly charged ion based TOF-SIMS contain chemical structure information. It has been suggested that atomic, positive secondary ions are formed primarily in the center of the impact area of highly charged ions, where the ionization density is highest. Complementary, large molecular ions and negative ions are emitted from the fringe of the interaction region. Emission of these ions has been proposed to result from a shockwave, following the rapid expansion of the highly ionized target volume in a Coulomb explosion.^{9,19} In addition, negative ions can also be formed by electron capture. The contribution to secondary ion production from conventional collisional momentum transfer was investigated *in situ* using a beam of charge state equilibrated $\text{Xe}^{q=q_{eq}}$ ions with $q_{eq} \approx 1.5+$, at ~ 2 keV/u. Charge equilibration was achieved by passing Xe^{44+} ions through a 10 nm thick carbon foil. The resulting flight time spectrum of negative secondary ions from a 50 nm thick thermal SiO₂/Si target is shown in Fig. 2(a). Secondary ion count rates increase by over two orders of magnitude when the high charge of primary ions, here Xe^{44+} , takes effect [Fig. 2(b)]. The increase of the number of molecular ions produced per incident projectile was found to scale with primary ion charge, $\sim q^n$, $n=3-4$.⁹ Figure 2(c) shows a negative secondary ion spectrum from a 50 nm thick B-SiO₂ target, taken before the first Ar-sputter cycle. Probe ions were Xe^{44+} at 3.2 keV/u. The dose was only 4.6×10^5 Xe^{44+} ions. SiO₂⁻ and SiO₃⁻ and (SiO₂)_nO⁻-cluster series are molecular ions characteristic for thermal SiO₂ films.⁹ The BO₂⁻ peak and an increased fraction of SiO⁻ reflect incorporation and chemical bonding of boron at high concentrations in the SiO₂ matrix. Typical sputter ion yields of molecular ions in standard SIMS are $\leq 10^{-3}$. Here, 6.5×10^{-3} BiO₂⁻ molecules were detected per Xe^{44+} . This count rate does not include the overall transmission of the instrument of $\sim 10\%$. Monitoring of both atomic and molecular secondary ions in highly charged ion based TOF-SIMS allows for simultaneous determination of the concentrations of impurities and the chemical structure of materials.

Both positive and negative secondary ion yields were

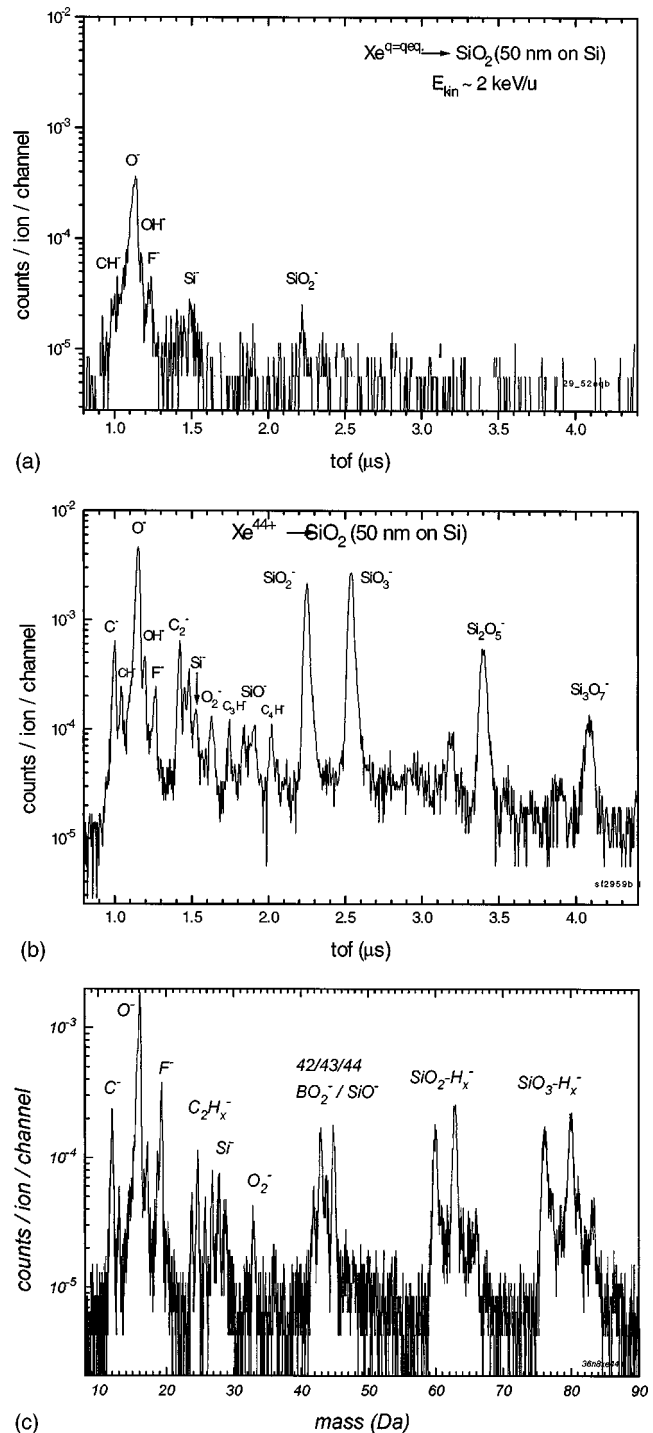


Fig. 2. Negative secondary ion spectra from thermal SiO₂ (50 nm on Si) at impact of xenon ions in charge state equilibrium, (a) and at impact of Xe^{44+} ions at the same kinetic energy (b). Negative secondary ion spectra from as-received 50 nm thick B-SiO₂/Si films at impact of Xe^{44+} ions. The primary ion dose was 4.6×10^5 .

found to decrease strongly with decreasing oxide thickness after consecutive Ar-sputtering cycles (Fig. 3). This effect is in accordance with ion yield measurements from silicon oxides of different thicknesses.^{16,20} Electron transport from the silicon substrate to the highly ionized surface region can quench a fraction of the Coulomb stress and reduce the mag-

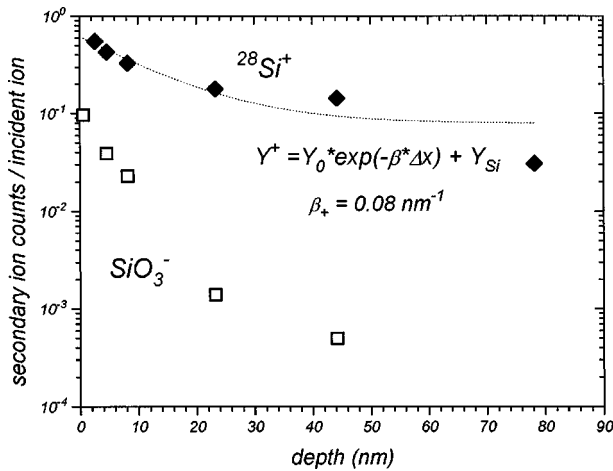


FIG. 3. SiO₃⁻ (□) and ²⁸Si⁺ (◆) yields from a B-SiO₂/Si film as a function of sample depth. The fit is a least square fit to an exponential dependency of the ²⁸Si⁺ yield on oxide thickness. The initial oxide thickness, as determined by RBS, was 50 nm.

nitude of secondary particle emission in electronic sputtering events. A fit to an exponential dependency on oxide thickness, Δx , yields an estimate of a materials parameter β (nm⁻¹):

$$Y^{\pm} = Y_0 \exp(-\beta \cdot \Delta x) + Y_{Si}, \quad (1)$$

(Y^{\pm} , positive or negative secondary ion yield; Y_0 , ion yield from thick oxide; Y_{Si} , ion yield from silicon substrate). β reflects the quenching of the induced Coulomb stress at the surface by substrate electrons. Values are found to be larger for negative cluster ions ($\beta_{-} \approx 0.2 \text{ nm}^{-1}$) than for positive atomic ions ($\beta_{+} \approx 0.08 \text{ nm}^{-1}$). This observation indicates different quenching characteristics of primary and secondary (i.e., shock waves¹⁹) Coulomb explosion effects, the detailed understanding of which is subject of ongoing studies.

IV. CONCLUSION

We have shown that electronic sputtering induced by slow, highly charged ions like Xe⁴⁴⁺ or Th⁷⁰⁺ can be employed for quantitative materials analysis. Boron concentrations of PE-CVD B-SiO₂ films in the $2 \times 10^{21} \text{ atoms/cm}^3$ range have been determined in agreement with independent measurements by ERD. High yields of positive and negative secondary ions in highly charged ion based SIMS allow for surface characterization with very low ($\leq 5 \times 10^5$) primary ion doses. The indicated strong de-coupling of positive secondary ion production probabilities from elemental ionization potentials enables the quantitative analysis of surface near layers without distortions due to surface transients, i.e., before sputter beam and target have been equilibrated.

ACKNOWLEDGMENTS

The authors thank Dr. D. L. Phinney (LLNL) for the performance of the standard SIMS measurements. One of the authors (T.S.) would like to thank Professor Dr. K. Bethge and Professor Dr. H. Schmidt-Böcking (Goethe Universität, Frankfurt) for their continuous support. This work was performed under the auspices of the U. S. Department of Energy by Lawrence Livermore National Laboratory under Contract No. W-7405ENG-48.

- ¹K. Wittmaack, in *Inelastic Ion Solid Collisions*, edited by N. H. Tolk, J. C. Tully, W. Heiland, and C. W. White (Academic, New York, 1977), p. 153.
- ²For a recent discussion see, L. A. Heimbrook, F. A. Baiocchi, T. C. Bitter, M. Geva, H. S. Luftman, and S. Nalohara, *J. Vac. Sci. Technol. B* **14**, 202 (1996); J. W. Erickson and R. Brigham, *ibid.* **14**, 353 (1996).
- ³M. Haag, H. Gnaser, and H. Oechsner, *Fresenius J. Anal. Chem.* **353**, 565 (1995).
- ⁴H. F. Arlinghaus and C. F. Joyner, *J. Vac. Sci. Technol. B* **14**, 294 (1996).
- ⁵C. He, J. N. Basler, and C. H. Becker, *Nature (London)* **385**, 797 (1997).
- ⁶J. L. Hunter and S. F. Corcoran, *J. Vac. Sci. Technol. A* **8**, 2323 (1990).
- ⁷A. Schnieders, R. Möllers, M. Terhorst, H.-G. Cramer, E. Niehuis, and A. Benninghoven, *J. Vac. Sci. Technol. B* **14**, 2712 (1996).
- ⁸See, for example, P. K. Chu and S. L. Grube, *Anal. Chem.* **57**, 1071 (1985).
- ⁹T. Schenkel, M. A. Briere, H. Schmidt-Böcking, K. Bethge, and D. Schneider, *Phys. Rev. Lett.* **78**, 2481 (1997); T. Schenkel, A. V. Barnes, M. A. Briere, A. Hamza, A. Schach von Wittenau, and D. H. Schneider, *Nucl. Instrum. Methods Phys. Res. B* **125**, 153 (1997); T. Schenkel, M. A. Briere, A. Schach von Wittenau, and D. Schneider, Proceedings of the 43rd ASMS Conference, May 1995, Atlanta, p. 1336; T. Schenkel, M. A. Briere, H. Schmidt-Böcking, K. Bethge, and D. Schneider, *Mater. Sci. Forum* **248-249**, 413 (1997).
- ¹⁰D. H. Schneider and M. A. Briere, *Phys. Scr.* **53**, 228 (1996); G. Schiwietz, M. Briere, D. Schneider, J. McDonald, and C. Cunningham, *Nucl. Instrum. Methods Phys. Res. B* **100**, 47 (1995).
- ¹¹D. Schneider *et al.*, *Phys. Rev. A* **42**, 3889 (1990).
- ¹²Y. Yamamura and H. Tawara, *At. Data Nucl. Data Tables* **62**, 149 (1996); G. Betz and G. K. Wehner, in *Sputtering by Particle Bombardment II*, edited by R. Behrisch (Springer, Berlin, 1983), p. 11.
- ¹³J. A. Knapp, J. C. Barbour, and B. L. Doyle, *J. Vac. Sci. Technol. A* **10**, 2685 (1992).
- ¹⁴K. Iltgen, C. Bendel, A. Benninghoven, and E. Niehuis, *J. Vac. Sci. Technol. A* **15**, 460 (1997).
- ¹⁵M. Sporn, G. Libiseller, T. Neidhart, M. Schmid, F. Aumayr, H. P. Winter, P. Varga, M. Grether, D. Niemann, and N. Stolterfoht, *Phys. Rev. Lett.* **79**, 945 (1997); T. Schenkel *et al.* (to be published).
- ¹⁶T. Schenkel, Ph.D. thesis, J. W. Goethe Universität, Frankfurt, Germany, 1997.
- ¹⁷S. W. Novak and R. G. Wilson, *J. Appl. Phys.* **69**, 463 (1991); *ibid.* **69**, 466 (1991).
- ¹⁸J. A. Knapp, J. C. Banks, and B. L. Doyle, *Nucl. Instrum. Methods Phys. Res. B* **85**, 20 (1994).
- ¹⁹I. S. Bitsensky and E. S. Parilis, *Nucl. Instrum. Methods Phys. Res. B* **21**, 26 (1987); R. E. Johnson, B. U. R. Sundqvist, A. Hedin, and D. Fenyö, *Phys. Rev. B* **40**, 49 (1989).
- ²⁰M. A. Briere, T. Schenkel, and D. H. Schneider, EBIT Annual Report 1994, LLNL, UCRL-ID-121572, p. 38 (unpublished).